COMPUTERS AND ELECTRONICS IN AGRICULTURE 60 (2008) 178–189

available at www.sciencedirect.com

ScienceDirect

journal homepage: www.elsevier.com/locate/compag

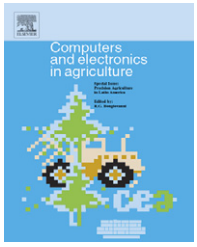

Hardware and software efficacy in assessment of fine root diameter distributions

*Richard W. Zobel**

USDA-ARS-AFSRC, 1224 Airport Road, Beaver, WV 25813-9423, United States

ARTICLE INFO

Article history:
Received 22 January 2007
Received in revised form
24 July 2007
Accepted 5 August 2007

Keywords:
Fine roots
High resolution
Scanner
Digital image analysis
Diameter distribution
Root length

ABSTRACT

Fine roots constitute the majority of root system surface area and thus most of the nutrient and water absorption surface. Fine roots are, however, the least understood of all plant roots. A sensitivity analysis of several software programs capable of providing root diameter distribution analyses was undertaken to determine if this software was capable of discriminating 10% changes in diameters of roots in the 0.05–0.2 mm diameter range. Digital images produced by drawing discrete lines, by scanning wires of various diameters, and by scanning roots from several legume species were analyzed and compared. None of the three packages were able to adequately analyze these images. Each introduced artifacts into the data that were severe enough to confound interpretation of the resulting diameter class length histograms at resolutions from 24 to 400 pixels (px) mm^{-1}, and root diameters from 0.06 to 0.5 mm or larger. One package was, however, clearly superior to the other two for routine digital analysis. All three packages require additional development before they are suitable for routine analysis of fine roots. Due to the 252 px mm^{-1} resolution ceiling with currently available scanners, the smallest roots for which this level of discrimination is possible is 0.12 mm diameter. For many agricultural and forest species, up to 95% of their total root length is less than 0.1 mm in diameter. It is concluded that both hardware and software constraints currently inhibit the sensitivity of investigations into fine root diameter shifts in response to environmental conditions.

Published by Elsevier B.V.

1. Introduction

Fine roots (up to 95% of root system length) are the primary source of water and nutrients for plant growth and development. Although the classic description of the fine root class states that they are those roots less than 2 mm in diameter (Böhm, 1979), most fine roots are much smaller. In the literature, fine roots of hardwoods, crop species, forages, and weeds have been measured down to 0.06 mm diameter (Lyford, 1975; Wright et al., 1999; Zobel, 2005). The fine root classification lumps 95% of plant root length into one generic classification without a demonstration of their physiological or developmental similarity.

Zobel et al. (2006) demonstrated that in chicory, the fine roots can display three different cultivar dependent responses to phosphorus deprivation: first, a reduction in length of one diameter class cluster of fine roots in favor of a second, thinner diameter class cluster; second, a reduction in fine root mass density without a concomitant change in length; third, the reverse of the first type of response. In the first response type, the larger roots averaged 0.86 mm diameter, and the smaller averaged 0.28 mm diameter (approximately 75% of total root length). The images, from which these data were taken, were photographed at 317 dpi (12.5 px mm^{-1}), and, with the diameter class length plotted against a diameter class log scale, the polygonal histogram displayed dips/humps in the curve, sug-

* Tel.: +1 304 256 2825; fax: +1 304 256 2921.
E-mail address: rich.zobel@ars.usda.gov.
0168-1699/$ – see front matter. Published by Elsevier B.V.
doi:10.1016/j.compag.2007.08.002

gestive of distinct diameter class clusters. Two of these humps appeared to correspond with the 0.28 and 0.86 mm diameter class clusters. Similar dips and humps in histograms have been observed with three other species (Zobel, 2005).

The finest roots (0.28 mm diameter) in the Zobel et al. (2006) data averaged 3.5 pixels in diameter. This resolution is, then, slightly below the threshold suggested by Zobel (2003) as that needed to accurately identify distinct roots. Using Zobel's (2003) rule of pixel size needing to be 25% or less than the diameter of the smallest root for accurate identification, a minimum imaging resolution of 0.015 mm (67 px mm^{-1} or 1700 dpi) would have been needed to accurately identify these roots. Subsequent studies of the three chicory cultivars in soil (pots) and field conditions confirm the observations of Zobel et al. (2006), and extend them by demonstrating that the finest roots also change in diameter in response to changes in phosphorus (Zobel, unpublished data).

Ryser and Lambers (1996) and Ryser (1998; cf. p. 452—Fig. 7) present several root histograms that appear to show shifts in *Dactylis glomerata* L. (Orchardgrass, OG) and *Brachypodium pinnatum* (L) Beauv. (Heath False Brome, HFB) root diameter with shifts in nutrient level. These apparent shifts are on the level of 10–30% of the nominal diameter of the roots. Since OG and HFB both have the majority of their fine roots in the 0.1 mm diameter range in field grown plants, a 10% shift in diameter (0.01 mm × 0.25 = 0.0025 mm) requires an optimum resolution of 400 px mm^{-1}. The best resolution for scanners in reasonable price ranges is currently 252 px mm^{-1}. From a visual interpretation of the Ryser (1998) histograms, it might be suggested that OG fine roots become thicker with increased nitrogen, while HFB initiates a new, additional, diameter class of root (approximately 30% larger) with increased nitrogen. Either pattern would require discrimination at the 133 px mm^{-1} resolution level. For species with fine roots in the 0.06 mm diameter range, the required resolution would be on the order of 222 px mm^{-1}, minimum, for a 30% change in diameter. Zobel et al. (2007) demonstrate fine root diameter shifts with changes in nutrient concentration for 12 different species. In their data the diameter shifts averaged 20–25% of the diameter at the lowest concentration. Diameters of the fine roots of the 12 species ranged from 0.07 to 0.27 (Zobel et al., 2007). If shifts in diameter are ubiquitous responses to changes in root environment, as suggested by Zobel et al. (2007), rhizobotanical research will need scanners with significantly higher resolutions, and software capable of analyzing the resultant images.

There are many software packages capable of assessment of root length and average diameter from scan or photograph images. However, very few packages assess the allocation of root length amongst diameter classes down to the pixel level. If root diameter is a continuous variable and roots of different diameter are physiologically identical, this does not matter, but as seen in the Zobel et al. (2006) analysis and as suggested by the data in the Cahn et al. (1989), McCully (1987), Varney et al. (1991), Ryser (1998) and Zobel et al. (2007) research, root diameter is probably not a continuous variable and root physiology may differ with diameter class. The working hypothesis in this laboratory is: root diameter is a discontinuous variable with different meso-diameter classes (clusters of adjoining diameter classes) having distinctly different functional patterns. Roots initiated and growing at different times during the life cycle of a root system will have different diameters due to differences in their growing conditions, and life cycles. If analysis is not carried out at a high enough resolution, such a situation would give rise to an apparent continuous distribution that masks the underlying sets of discontinuous distributions. This leads to the conclusion that for detection and analysis of a discontinuous root diameter distribution, researchers need imaging technology and software capable of dissecting root diameter into diameter classes well into the micron sized pixel range.

Two software packages [WinRhizo v. 2005b (regent.qc.ca) and Delta-T Scan v 2.0 (delta-t.co.uk)] report results as diameter class length, with diameter class set by the user (from multiple pixels per diameter class to actual pixel size/density). Delta T Scan is a legacy software that runs under DOS. Bouma et al. (2000) treated these two commercial packages to a sensitivity analysis of their ability to measure root length and diameter distribution. Their results conclude that the two packages are effectively equivalent and do a good job of assaying diameter distribution. Unfortunately, the highest resolution used in the Bouma et al. (2000) study was 19 px mm^{-1}. According to the analysis by Zobel (2003), this resolution restricts root separation and detection to roots greater than 0.21 mm diameter. A third package, Image Processing Tool Kit (reindeergraphics.com), has several routines that can be combined to give assessments of root length and diameter. One set thins the image to a single pixel thick line then assesses the distance from the line to the edge. Although it does this on a pixel-by-pixel basis, it reports the results as a root segment ("feature") length and mean radius with standard deviations. WinRhizo also uses thinning with threshold edge discrimination, while the actual process used by Delta T Scan is unclear.

The following research is an attempt to test a hypothesis for the most extreme case: existing available hardware and software can detect 10% diameter shifts in roots of 0.06 mm diameter. If this hypothesis is validated, it can logically be assumed that shifts in diameter of larger roots can also be documented. It can be argued that analysis of precise lines of a given thickness is not comparable to the analysis of inherently variable roots. However, any software claiming to be accurate in the assessment of root diameter must be extremely accurate with images with little or no inherent variability. Therefore, in an attempt to determine if current diameter class assessing software were up to the tasks outlined above, we constructed a series of straight lines at many angles and with specific uniform thicknesses. We then analyzed these lines to determine software suitability. This was followed by an assessment of scanned images of wires and roots.

2. Materials and methods

Two different computer systems were used: a Dell[1] Optiplex GX270 with a Pentium 4 at 3.2 GHz with 2 GB RAM, running Windows XP Professional (DELL) and a 2.5 GHz Power Mac G5

[1] Reference to a manufacturer or trademark is solely for the reference of the reader and is not a recommendation by the USDA.

Table 1 – Comparison of analysis packages

Software	Computer type	Operating system	Image type	Maximum file size (MB)
WinRhizo	PC	Windows	Color/grayscale	>150
Delta-T Scan	PC	DOS	Bit map	<50
IPTK	PC/MAC	Photoshop	Color/grayscale	<30

quad Intel CPU with 4 GB RAM, running OS X 10.4.8 (MAC). An Epson Expression 4990 (4800 hardware dpi – 189 px mm^{-1} – Epson.com), attached to the DELL, was used to scan in the wires and roots. All scanned images were made using the transparency adapter to eliminate wire shine, and root color effects. This might decrease precision of root diameter assessment (roots were washed then imaged, without staining) of translucent roots, but any effect would be independent of actual diameter and resolution used.

Four Software packages were used: WinRhizo, v 2005b (regent.qc.ca) running on the DELL (WR)—routine settings were diameter interpolation, maximum diameter sensitivity, and automatic thresholding; Delta-T Scan v 2.0 (delta-t.co.uk) running on the DELL in DOS mode (DT)—DT resolution was routinely set at 100 dpi and analysis carried out in the sine theta mode. An appropriate multiplier was used to convert the results to the appropriate image resolution values. Image Processing Tool Kit (IP) 5.0 (Reindeergraphics.com) running within Photoshop—a thinning with Euclidean Distance Mapping (IP) procedure was used; and Photoshop CS (v. 8) (Adobe.com) running on the MAC. Table 1 compares some of the more major characteristics among these analysis programs. Results are commonly expressed as total length of root within each diameter class (DCL). WR commonly reports this as centimeters, and DT and IP report it as millimeters. IP, however, reports the results as a radius rather than a diameter. DT and WR report total length and average diameter (width) in the image as separate values. Since each software package operates primarily by analyzing pixels, their efficacy should be image resolution independent. For easy reference by the reader, Table 2 presents the conversion from popular dots per inch (dpi) to SI units (px mm^{-1} = dpi/25.4). Table 3 presents a brief table of data organized similar to that in WR output.

2.1. *Line images*

Images composed of lines of various thickness were generated in Photoshop at 94 and 189 px mm^{-1}. Images were initially drawn in bit map format, and converted to 8-bit grayscale for rotation to different angles. The image interpolation used for the grayscale rotation was "bicubic (better)". For DT, Photoshop was used to bi-level threshold (at a level of 128) the grayscale images into bit map mode prior to analysis.

The actual width of rotated lines was calculated by zooming in on the thresholded (128 or other levels as appropriate) image in Photoshop, and counting the pixels along the *x*- and *y*-axes from one side of the line to the other, and calculating the line width (w) by formula 4 or 5 (derived from the Pythagorean Theorem assuming the relationships shown in Fig. 1):

$$Z = (x^2 + y^2)^{0.5} \tag{1}$$

$$a = (w^2 - x^2)^{0.5}, \qquad b = (w^2 - y^2)^{0.5} \tag{2}$$

$$\text{if } Z = a + b \quad \text{then } (x^2 + y^2)^{0.5} = (w^2 - y^2)^{0.5} + (w^2 - x^2)^{0.5} \tag{3}$$

$$\text{solving for } w = \frac{xy}{(x^2 + y^2)^{0.5}} \tag{4}$$

$$\text{if } x = y \quad \text{then } w = \frac{x^2}{(2x^2)^{0.5}} = \frac{x}{2^{0.5}} = 0.707x \tag{5}$$

Eq. (4) is the general equation for estimating diameter by counting *x* and *y* pixels, while Eq. (5) is the reduced model for the perfect 45° angle case.

Table 2 – Conversion table for resolutions (dpi to px mm^{-1}), pixel size, and 10% change in line width for three different widths

dpi	px mm^{-1}	pixel size (mm)	10% of 0.4 mm (px)	10% of 0.1 mm (px)	10% of 0.06 mm (px)
300	12	0.0847	0.5	0.1	0.07
600	24	0.0423	0.9	0.2	0.14
635	25	0.0400	1.0	0.3	0.15
1, 200	47	0.0212	1.9	0.5	0.28
1, 270	50	0.0200	2.0	0.5	0.30
2, 400	94	0.0106	3.8	0.9	0.57
2, 540	100	0.0100	4.0	1.0	0.60
3, 600	142	0.0071	5.7	1.4	0.85
4, 800	189	0.0053	7.6	1.9	1.13
6, 350	250	0.0040	10.0	2.5	1.50
6, 400	252	0.0040	10.1	2.5	1.51
9, 600	378	0.0026	15.1	3.8	2.27
10, 160	400	0.0025	16.0	4.0	2.40
25, 400	1000	0.0010	40.0	10.0	6.00

Table 3 – Example data table derived from WR analysis of line set 1

Line width (px)	Angle	Total length (cm)	Average diameter (mm)	Diameter class length (cm)					
				DC = 0.011 mm	DC = 0.021 mm	DC = 0.032 mm	DC = 0.042 mm	DC = 0.053 mm	DC = 0.063 mm
1	0	1.058	0.011	1.0583	0	0	0	0	0
1	30	1.040	0.014	0.9073	0.1324	0	0	0	0
2	0	1.057	0.021	0.0011	1.0562	0	0	0	0
2	30	1.040	0.023	0.6202	0.4195	0	0	0	0
3	0	1.058	0.032	0	0.0021	1.0562	0	0	0
3	30	1.040	0.033	0	0.5611	0.4786	0	0	0
4	0	1.057	0.042	0	0.0011	0	1.0562	0	0
4	30	1.040	0.044	0	0.0030	0.4652	0.5715	0	0
5	0	1.058	0.053	0	0	0.0021	0	1.0562	0
5	30	1.041	0.054	0	0.0030	0	0.9318	0.1065	0
6	0	1.057	0.064	0	0	0.0011	0	0.0021	1.0541
6	30	1.040	0.065	0	0.0022	0	0.0015	0.5116	0.5244
Combined length				2.5869	2.1806	2.0032	2.561	1.6764	1.5785
Line width (px)	Angle	Summed length	Calculated diameter	Diameter class × diameter class length					
1	0	1.058	0.011	0.01120	0	0	0	0	0
1	30	1.040	0.012	0.00960	0.00280	0	0	0	0
2	0	1.057	0.021	0.00001	0.02236	0	0	0	0
2	30	1.040	0.015	0.00656	0.00888	0	0	0	0
3	0	1.058	0.032	0	0.00004	0.03353	0	0	0
3	30	1.040	0.026	0	0.01188	0.01520	0	0	0
4	0	1.057	0.042	0	0.00002	0	0.04471	0	0
4	30	1.040	0.038	0	0.00006	0.01477	0.02419	0	0
5	0	1.058	0.053	0	0	0.00007	0	0.05589	0
5	30	1.041	0.043	0	0.00006	0	0.03945	0.00564	0
6	0	1.057	0.063	0	0	0.00003	0	0.00011	0.06694
6	30	1.040	0.058	0	0.00005	0	0.00006	0.02707	0.03330

Diameter class (width class, DC) lengths are placed under their respective diameter class. The product of diameter class length by diameter class, and calculated diameter are also presented in the second half of the table.

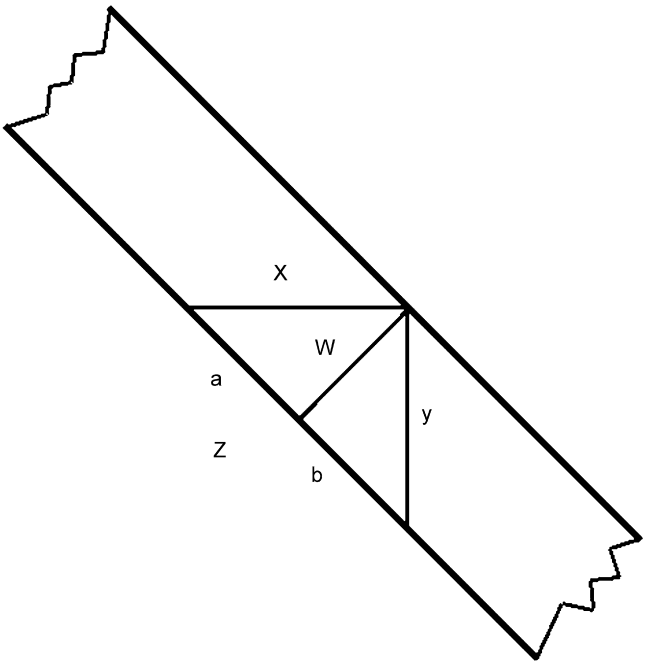

Fig. 1 – Diagrammatic representation of a piece of root imaged for analysis. The figure shows the *x*- and *y*-axis directions, the resulting *Z* and *w* (the perpendicular from the *x*, *y* angle to the *Z* hypotenuse).

The first set of lines at 189 px mm^{-1} (4800 dpi) from 1 to 30 pixels thick and 1 cm long, were drawn in vertical orientation, one line per image, then rotated to 5°, 10°, 15°, and so on up to 45° and saved as grey scale images in tiff format (a total of 300 images). A second set of lines was constructed by taking the 20 pixel thick vertical line and rotating it in 1° increments, for 46 different lines from vertical to 45°. These sets of lines were analyzed with WR, IP and DT.

A third set of lines, from 1 to 30 pixels thick, 1000 pixels long, and rotated to all angles from 0° (vertical) to 45° from vertical, was constructed at 94 px mm^{-1} (1380 single line images). These lines were then analyzed with WR only (see Section 4 for the rationale for only using WR).

Combined plots were prepared by summing, for each width class, the width class lengths amongst the nominal line widths and their angles of rotation. For WR and DT, calculated average line width (wire or root diameter) is found by multiplying the width class value by the width class length for that width class, followed by summing these products for the whole line and dividing by the total length (see Table 3).

2.2. *Wire images*

Wire pieces of different diameter and lengths were measured with a caliper (Table 2) then scanned at 94 px mm^{-1}, first as groups of approximately parallel wires of identical diameter, then as a mixture of all the wires with crossovers, etc. Separate scans were made with the mixture rotated roughly 22.5°, 45° and 67.5° from the original orientation. These images were then analyzed with WR. In addition, the original mixture image was rotated to 5°, 10°, 15°, and so on up to 45° and analyzed.

2.3. *Root images*

As a further assessment, four randomly chosen images from a set of 314 root images scanned in (94 px mm^{-1}) from an experiment utilizing 10 different legume species and three concentrations of phosphorus were analyzed by WR. Because of the relatively high resolution, the original set of roots was scanned in as 4 non-overlapping 10 cm × 10 cm images from different regions of the scanner surface. In addition, the Legume303.tif image was analyzed with WR set at four different thresholds (128, 162 {the level used by WR for one of the four legume images}, 188 {the level used by WR for the other three images, including 303}, and 214).

3. Results

A preliminary study with images drawn at 400 px mm^{-1} (pixel size 0.0025 mm) demonstrated that only WinRhizo (WR) was able to analyze these constructed images (98.5–152 MB file sizes) (see Table 1), and then not in its best resolution mode—apparently there were memory constraints. On the same DELL computer, Delta-T Scan (DT) requires that the images be less than 50 MB in size and in bit-map mode, and Image Processing Tool Kit (IP), on the MAC, requires that the images be smaller than 30 MB in size.

The analysis of the first set of lines (30–189 px mm^{-1} lines at 10 angles) by each of the software packages produced noisy combined histograms (Fig. 2). The dips and peaks in these histograms (up to 20% deviation from expected) are infrequently coincident between software packages. These dips occur 4, 4 & 3 width classes apart in WR and show a similar pattern with DT and IP.

A histogram of the combined results from WR analyses for lines angled at 45° and with nominal widths of 14–20 pixels demonstrates that WR has estimated all line widths at 1 pixel less than actual (Fig. 3—this occurs when WR is in maximum

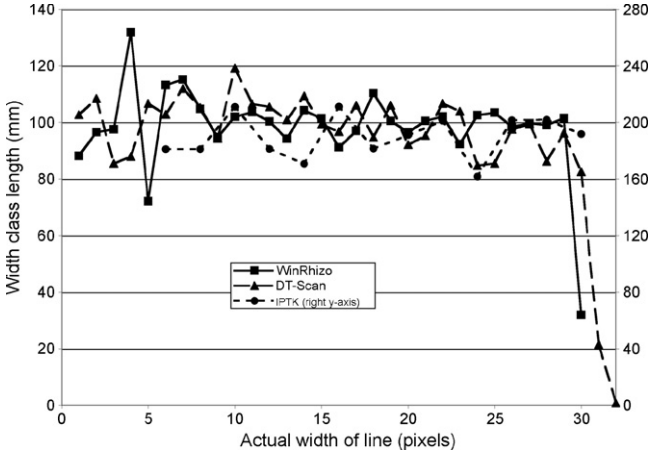

Fig. 2 – Histograms cumulative width class lengths of the 300 lines from line set one (30 line thicknesses—from 1 pixel to 30 pixels, each line thickness at 10 different angles—from 0° to 45° from vertical, resolution = 189 px mm^{-1}), analyzed with WinRhizo (WR), Delta T Scan (DT) and Image Processing Tool Kit (IP).

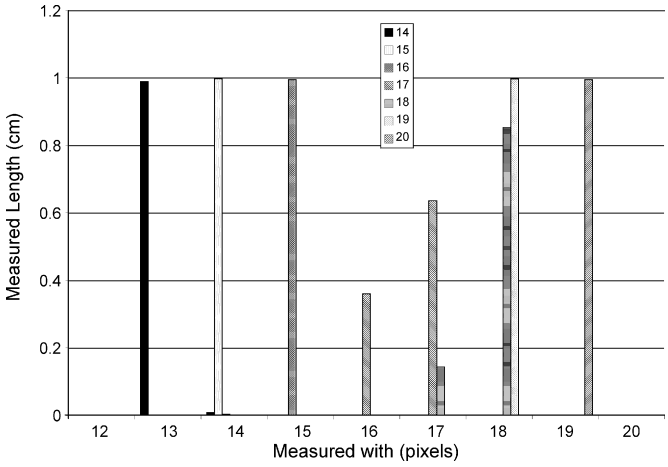

Fig. 3 – Bar graph of the WR analysis of seven 189 px mm^{-1} resolution lines (width 14–20 pixels). Nominal line length is 0.9991 cm per line.

diameter sensitivity mode), and that lines with a nominal thickness of 17 and 18 pixels are estimated to be of two thicknesses. Pixel counting confirms that the 17 and 20 pixel thick lines did change to two thicknesses with rotation, but the 18 pixel thick line did not (Table 4). DT and IP showed similar though not identical patterns, but also lost length to numerous smaller width classes (data not presented).

Taking a subset of lines from 15 to 20 pixels thick, and plotting the calculated average diameter against angle of rotation, for each software package, it is observed that angle of rotation affects the outcome (Fig. 4). After routinely adjusting the WR values up 1 pixel (adjusting for the observed down shift in Fig. 3), WR consistently reports the correct width with the vertical line, but reports thinner and thinner widths up to 25°. At 30–45°, WR reports a width 1 pixel smaller than actual with all but two classes (17 and 18 pixels thick—Fig. 4a). DT and IP also showed changes in reported width with changes in angle (Fig. 4b and c). DT data present a pattern similar to that of WR, but not as large a deviation from expected, and somewhat more irregular. IP on the other hand is very accurate at all angles with even numbered widths, but has up to a 2-pixel swing with odd numbered widths (Fig. 4c). IP is also missing the values for the 45° angle in the 15, 18, 19, and 20 pixel width lines.

Analysis reports for WR and DT contain an entry for total length and average diameter (Table 3). Total length can also be calculated by summing width class lengths, and average diameter can be calculated by multiplying each width class length by the value of the width class, summing these up and then dividing by total length (Tables 3 and 5).

Analysis of the second line set (46 angles with a 20 pixel width line at 189 px mm^{-1}) demonstrated an inconsistency with WR not found in the others (Fig. 5). For DT, calculated and average widths are identical, as are the total length and sum of width class lengths. For WR, the total and calculated lengths are identical, while the calculated average width (measured width—Fig. 5a) is not the same as the average width from the analysis report. From Fig. 5a, it can be seen that for WR, length changes slightly with changes in angle, while calculated diameter changes by a full pixel and average diameter has a full pixel swing. Diameter and length both vary with angle in the DT analysis, with length swinging from 2 mm below actual to 1.25 mm greater than actual with increasing angle from vertical (a 33% swing). There is comparatively little variation in either length or width in the 20 pixel IP analysis (Table 6), but the odd pixel thicknesses gave wide swings in width while producing less than a quarter mm divergence in length.

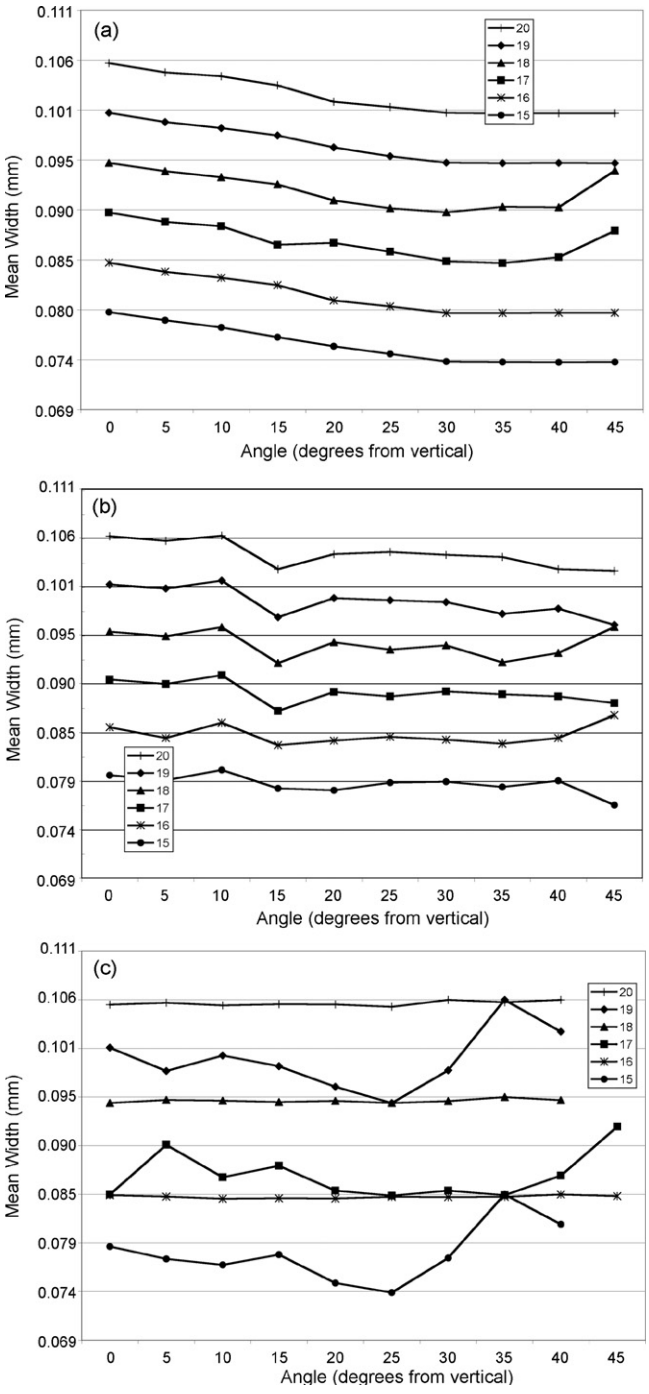

Fig. 4 – Plots of reported line width vs. line angle for six lines drawn at 189 px mm^{-1} and rotated at 10 different angles: (a) WR analysis; (b) DT analysis; (c) IP analysis.

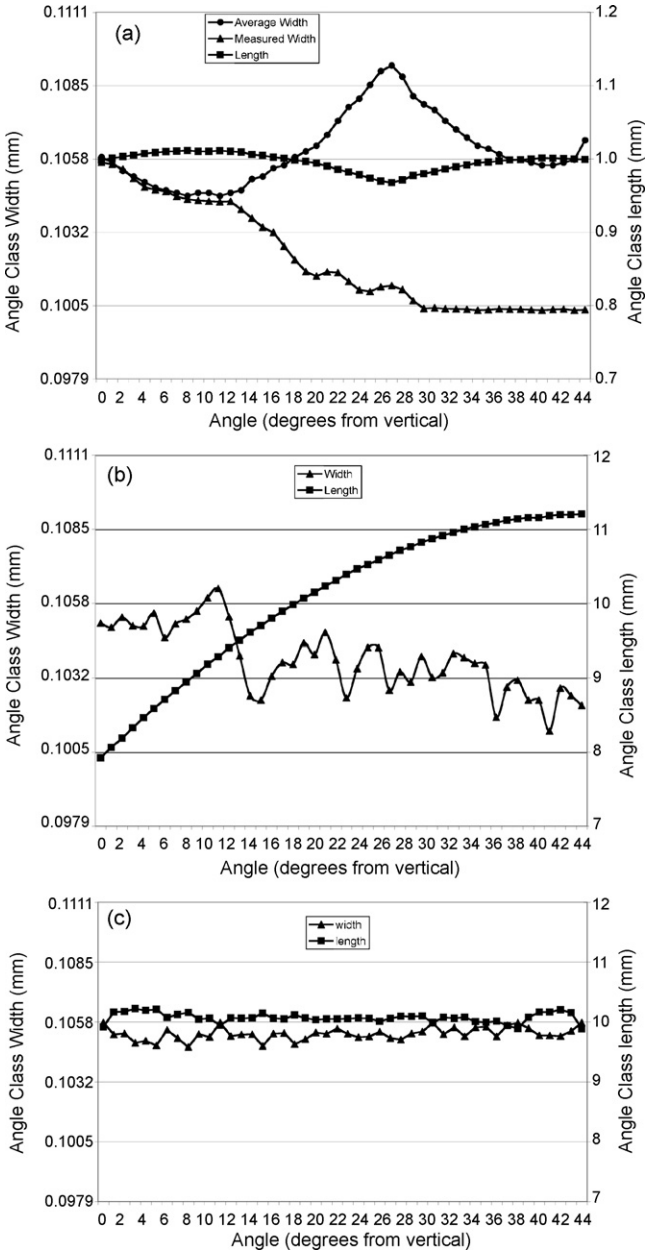

Fig. 5 – Plots of calculated angle class width and reported angle class length vs. angle of rotation for a 20 pixel (0.1058 mm, 19 pixels = 0.1005 mm) width line: (a) WR analysis (including reported average width); (b) DT analysis; (c) IP analysis.

The WR analysis of the third line set (94 px mm^{-1}) shows a similar pattern to that of the 189 px mm^{-1} s data set (data not shown). Fig. 6 presents a histogram of the combined data for the 30 line widths at 46 angles. The same types of dips and peaks as seen in the 189 px mm^{-1} data (Fig. 2) are present with a dip every third or fourth pixel. The dips in the 94 px mm^{-1} histogram at pixels 8 and 12 correspond in line width (mm) to the dips in the 189 px mm^{-1} histogram at pixels 16 and 23, respectively.

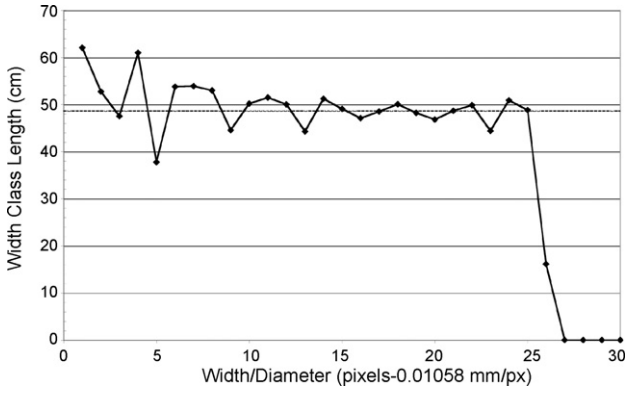

Fig. 6 – Histogram of cumulative WR reported width class lengths for constructed lines of 30 widths (from 1 to 30 pixels wide: 94 px mm^{-1}) rotated to 46 angles (0–45° from vertical). Width class lengths for a given width class are summed across all line widths and angles.

3.1. *Wires*

When the data from a WR analysis of the different sets of wires is combined, presented as a histogram, and compared to the histogram from a WR analysis of the mixed wires, the peaks in the mixed wire analysis are shifted down 1 or 2 pixels in the 0–0.45 mm diameter range (Fig. 7). When the threshold setting is changed from 128 to 214, the measured diameters of the mixed wires increased by 6 pixels (data not presented). Intermediate threshold values gave intermediate shifts.

When the parallel wire sets are imaged at different resolutions, wires with diameters that are closer together than the width of 1 pixel are pooled together (Table 7). The gap (difference in diameter) between 0.245 and 0.254 mm diameter wires is just 0.009 mm, and this difference is not recognized until the resolution is 142 px mm^{-1} (pixel size = 0.007 mm) or greater. The gap between 0.448 and 0.506 is 0.059 mm, but is not separated until a resolution of 94 px mm^{-1} is reached (pixel size of 0.011, <20% of the gap size) and the gap between 0.193

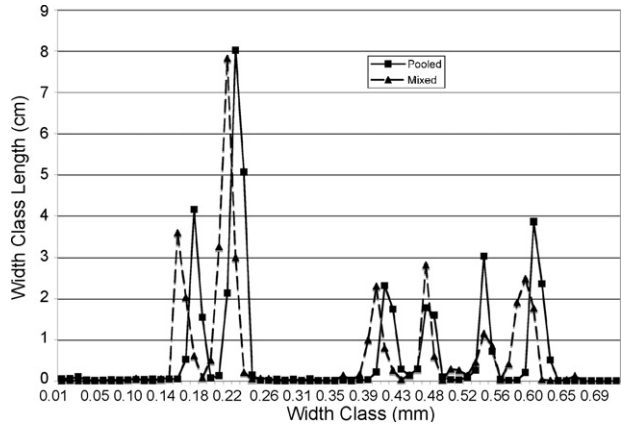

Fig. 7 – Histograms of the pooled diameter class length data, from WR analysis of seven images (94 px mm^{-1}) of parallel wires with uniform diameters, vs. diameter class and the WR analysis of the image (94 px mm^{-1}) of the same wires mixed together with wires crossing and touching.

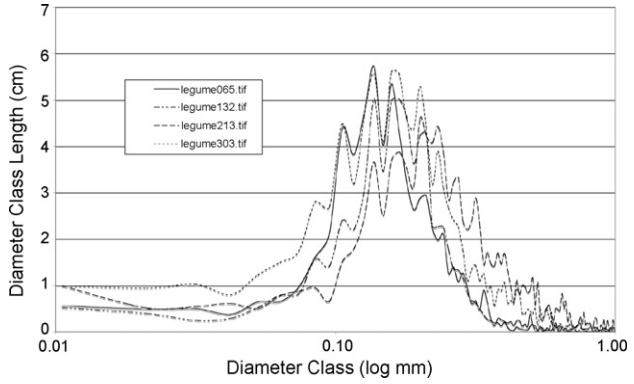

Fig. 8 – Histograms the diameter class length vs. diameter class from the WR analysis of four randomly chosen legume root images (94 px mm^{-1}) from a collection of 300+ images.

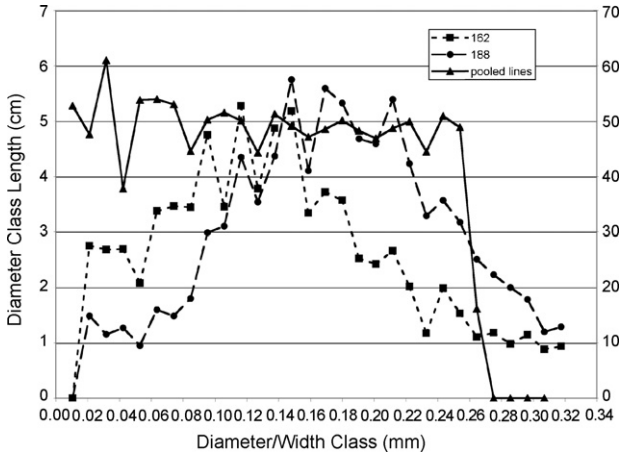

Fig. 9 – Composite plot of the histogram of the pooled WR analysis of line set 3 (Fig. 6—adjusted to the left 1 pixel) and histograms of the WR analysis of legume image 303 at thresholds of 162 and 188.

and 0.245 is 0.05 mm and the lowest resolution to discriminate this difference is 94 px mm^{-1} (0.011 mm or 22% of the gap). The WR reported diameters are consistently between 0.012 and 0.020 mm lower than actual. At 47 and 94 px mm^{-1}, this represents a 1-pixel shift (Fig. 3), but at 189 px mm^{-1} this represents up to a 4-pixel reduction in estimated diameter (8% of 0.245 mm and 23% of a 0.09 mm diameter root).

3.2. *Roots*

Histograms from a WR analysis of four legume root images (94 px mm^{-1}) show a series of coincident dips and peaks (Fig. 8). The four images were selected at random and represent different species. The average diameter differs among the images as does the total root length. The same coincident dips and peaks appear in all 314 image analyses. This type of coincident variation can only come from the scanner or the software. When Legume303 is analyzed with WR with the threshold set at different levels, the main peak shifts to the right with increasing threshold value, but the dips remain in the same position. This is shown for thresholds of 162 and 188 in Fig. 9 . The histogram of the combined analyses of line set 3 (adjusted 1 pixel to the left to account for the shift observed with parallel versus crossed wires—Fig. 8) demonstrates that the dips observed in the legume data occur at the same locations as that of the drawn line data. The dip at width class 12 (94 px mm^{-1}—Fig. 6) and width class 23 (189 px mm^{-1}—Fig. 2) correspond to the dip in the legume 303 histogram at diameter class 0.127 mm (Fig. 9).

4. Discussion

This research tests the hypothesis: existing available hardware and software can detect 10% diameter shifts in roots of 0.06 mm diameter. The conversion table (Table 2) demonstrates that a 10% shift in diameter of a 0.06 mm root (0.006 mm) is potentially detectable using a scanner resolution of 189 px mm^{-1} (pixel size 0.0053 mm). This is true only if it is assumed that variation in object diameter or measurement are not issues. Scanner imaging of even the most accurately constructed objects violates this assumption. Scanner sensors "see" in Color/color, and Grayscale images can become larger or smaller than actual when thresholded (becoming larger with increasing threshold value). Scanner bit mapped (black and white) imaging uses thresholding to determine the cut-off point for black versus white (a threshold is the level of grey [from 0 {black} to 255 {white} above which a pixel will be perceived as white]. The measured size of an object then is dependent on the threshold chosen by the operator or the software (as with WinRHIZO when set in automatic threshold mode). In addition, vertical smooth lines, or wires or roots, at angles other than vertical or horizontal (scanner bars and the attached image sensors are horizontal [*x*-axis] and the scan direction is vertical [*y*-axis]) are not smooth lines because the pixels that make up the image are represented as squares. This can result in a single line being represented by two or three diameter classes rather than just one (Fig. 3 i.e. 17 pixels wide ± 1 pixel when at 45°). If the study is to compare root systems of plants of two isolines or root systems of plants of a homozygous line treated to different conditions, the constraints are relaxed. In this case the roots appear in different images and curve modeling (i.e. non-linear regression) should be able to detect single pixel shifts between the histogram curve midpoints. This is essentially resolution invariant, so a 10% shift of a 0.06 mm diameter root (0.006 mm) would require a resolution of 167 px mm^{-1}, well within the range for currently available hardware.

Another potential scenario is suggested by the Ryser (1998, cf. p. 452—Fig. 7) Heath False Brome (*Brachypodium pinnatum* (L) Beauv) image. In this case, it can be speculated that an entirely new diameter class of roots has been initiated in response to the treatment conditions, such that two diameter classes are present. The close proximity of the diameter class midpoints apparently causes the two peaks to merge when the peak height of the smaller is quite small. To obviate overlap between peaks, a 10% shift in diameter would have to involve at least 3 pixels to avoid Thresholding/thresholding effects and pixel offsets which would cause overlap of peaks (1 pixel to either side of both diameter classes plus 1 pixel).

This requires a scanner resolution of 500 px mm^{-1} for scanning roots of 0.06 mm diameter (0.006 mm divided by 3 is 0.002 mm per pixel or 500 px mm^{-1}). The best available optical scanner resolution is 252 px mm^{-1} which (assuming a 10% shift in diameter and a 3 pixel extent of the shift) would translate to a root diameter of 0.12 mm (10% is 0.012 mm, divided by three is 0.004 mm per pixel or a resolution of 250 px mm^{-1}) as effectively the smallest root for which detecting a 10% shift in diameter is consistently possible. The validity of a 3 pixel diameter shift being required for measurement of a 10% shift is questioned by the observation that when WinRhizo estimates the diameters of wires, it fails to separate different diameters until the pixel size is 20% of the difference in diameter (i.e. a 5 pixel diameter shift—Table 7). Using this more restrictive case, the smallest diameter for which a 10% shift could be detected is 0.2 mm. The hardware portion of the hypothesis is invalid for these more stringent cases. Our research involves growing plants under one condition and then changing the conditions and detecting the time course of changes in root diameter and sites of initiation. This methodology requires the more stringent cases, therefore the hardware portion of the hypothesis is invalid.

The software component of the hypothesis is also problematic. Delta-T Scan is, effectively, legacy software that runs under DOS, and requires bit mapped (black and white) images. The former is inconvenient, but the later amplifies the thresholding problem by requiring the user to, more or less arbitrarily, select a threshold either before scanning, or after scanning and during image preparation for analysis. As has been discussed elsewhere, staining of roots can reduce (not eliminate) the thresholding problem (Bouma et al., 2000; Costa et al., 2001), but this is not a viable approach with live tissues to be used in further analyses or live plants to be grown further. A further difficulty is the 32.5% swing in estimated line length (Fig. 5b) with changing angle of orientation. This problem will become increasingly severe with the shorter and shorter segment lengths found in higher root density scanned images. For the purposes of detecting diameter shifts, the use of Delta-T Scan is effectively precluded.

Image Processing Tool Kit (IP) runs within Photoshop and is available for MAC and PC systems. IP, however, reports results as segment length and average diameter. This is not a difficulty with scanned images of excavated and washed roots. With intact root systems, IP will average the diameter of longer roots, much as with software like RootEdge (Kaspar and Ewing, 1997) and ImageJ (NIH, http://rsb.info.nih.gov/ij/) which were not considered here. IP does, internally, do a pixel-by-pixel (along the thinned length of the object/segment) assessment of radius, but only reports the averaged result with max/min and standard deviation. There is the potential, therefore, to develop a reporting method that gives true diameter class lengths. The ability to handle touching and crossing objects is, however, problematic. The most critical deficiency of IP is the inability to accurately measure width of objects with odd pixel widths (a 2 pixel swing with change in angle—Fig. 4c), and lack of analysis of all 45° angled lines. These two deficiencies currently preclude the routine use of IP for measurement of fine roots.

WinRHIZO (WR) is currently the most heavily used and apparently the most sophisticated root analysis software package (Himmelbauer et al., 2004; McPhee, 2005; Zobel, 2003). There are some critical deficiencies with this software package: width class is routinely shifted down 1 pixel from actual when used in its most sophisticated diameter assessment mode (Morphology: diameter interpolation: maximum precision—Fig. 3); the calculated measured width of a line decreases with increasing angle of orientation, up to 1 pixel from actual (Figs. 4 and 5); average line width varies with increasing angle of rotation (Fig. 5a) and the standard deviation of the mean across angle of rotation increases as actual width increases (Table 5); width class length varies with increasing angle of rotation (Fig. 5a), but standard deviation of the mean across angle of rotation is constant as width increases (Table 5); calculated width decreases with increasing angle of rotation (Fig. 5a) and the standard deviation of the mean across angle of rotation is relatively constant with increasing width (Table 5); finally, WR shifts measured low diameter wire widths down 1 or 2 pixels when the wires are mixed together with overlaps versus when scanned as individual sets of wires of different diameters (Fig. 7). Fortunately all these variations appear to be statistically negligible when considered separately.

The presence of rather large dips in the histograms from WR analyses (Figs. 2, 6, 8 and 9 see also Zobel et al., 2007 (Fig. 1) with dips in a 24 px mm^{-1} [600 dpi] image analysis) complicates interpretation of the histograms. This complication is especially severe if visual interpretation is used to determine if there is a shift in average diameter of roots. The estimate that detection of diameter shifts requires a resolution which provides 3 pixels within a space that is 10% of line width, con-

Table 4 – Measured (*x*-axis pixel counts times 0.707) and WR analyzed widths of seven lines (45° rotation—189 px mm^{-1})

Drawn width	x-Axis pixels	Measured width in pixels (threshold = 128)	WR reported width in pixels	WR threshold
14	20	14.4	13	121
15	21	14.85	14	121
16	23	16.26	15	131
17	24/25	16.97 (83%)/17.65 (17%)	16 (36%)/17 (64%)	132
18	26	18.38	17 (14%)/18 (86%)	129
19	27	19.09	18	109
20	28/29	19.76 (64%)/20.5 (36%)	19	131

Percentages are the percent of original length associated with the determined width class.

Table 5 – WR estimated line length, average and calculated diameters (with standard deviations) averaged across 10 angles of rotation for lines drawn with a resolution of 189 px mm^{-1} and thicknesses from 1 to 30 pixels

Line width		Length (cm)			Average diameter			Calculated diameter		
Pixels	mm	Average (cm)	S.D.		Average (mm)	S.D.		Average (mm)	S.D.	
			mm	Pixels		mm	Pixels		mm	Pixels
1	0.0053	0.9188	0.2114	399.50	0.0069	0.00086	0.16	0.0060	0.00055	0.10
2	0.0106	0.9963	0.0117	22.16	0.0114	0.00066	0.12	0.0085	0.00148	0.28
3	0.0159	0.9980	0.0119	22.49	0.0165	0.00081	0.15	0.0143	0.00124	0.24
4	0.0212	0.9968	0.0117	22.19	0.0215	0.00041	0.08	0.0197	0.00095	0.18
5	0.0265	0.9978	0.0120	22.76	0.0266	0.00035	0.07	0.0233	0.00206	0.39
6	0.0317	0.9976	0.0117	22.11	0.0321	0.00067	0.13	0.0301	0.00102	0.19
7	0.0370	0.9987	0.0125	23.58	0.0372	0.00051	0.10	0.0349	0.00145	0.27
8	0.0423	0.9980	0.0120	22.66	0.0424	0.00069	0.13	0.0389	0.00230	0.43
9	0.0476	0.9978	0.0122	23.03	0.0479	0.00064	0.12	0.0442	0.00216	0.41
10	0.0529	0.9968	0.0118	22.37	0.0530	0.00071	0.13	0.0499	0.00173	0.33
11	0.0582	0.9980	0.0119	22.58	0.0582	0.00086	0.16	0.0547	0.00213	0.40
12	0.0635	0.9973	0.0119	22.40	0.0638	0.00078	0.15	0.0600	0.00211	0.40
13	0.0688	0.9964	0.0118	22.29	0.0691	0.00089	0.17	0.0653	0.00211	0.40
14	0.0741	0.9975	0.0116	21.97	0.0744	0.00087	0.17	0.0708	0.00192	0.36
15	0.0794	0.9972	0.0119	22.51	0.0795	0.00100	0.19	0.0759	0.00203	0.38
16	0.0847	0.9976	0.0116	21.98	0.0848	0.00100	0.19	0.0811	0.00206	0.39
17	0.0899	0.9972	0.0120	22.70	0.0903	0.00109	0.21	0.0868	0.00187	0.35
18	0.0952	0.9977	0.0119	22.50	0.0957	0.00126	0.24	0.0922	0.00199	0.38
19	0.1005	0.9976	0.0120	22.68	0.1008	0.00121	0.23	0.0970	0.00205	0.39
20	0.1058	0.9962	0.0117	22.13	0.1062	0.00124	0.23	0.1022	0.00209	0.39
21	0.1111	0.9965	0.0121	22.79	0.1113	0.00143	0.27	0.1077	0.00191	0.36
22	0.1164	0.9958	0.0120	22.71	0.1167	0.00143	0.27	0.1129	0.00205	0.39
23	0.1217	0.9971	0.0120	22.64	0.1218	0.00164	0.31	0.1181	0.00202	0.38
24	0.1270	0.9973	0.0121	22.84	0.1274	0.00157	0.30	0.1237	0.00200	0.38
25	0.1323	0.9966	0.0121	22.91	0.1330	0.00173	0.33	0.1289	0.00189	0.36
26	0.1376	0.9954	0.0115	21.77	0.1381	0.00162	0.31	0.1339	0.00199	0.38
27	0.1429	0.9967	0.0117	22.18	0.1432	0.00172	0.33	0.1392	0.00210	0.40
28	0.1481	0.9962	0.0120	22.59	0.1484	0.00178	0.34	0.1444	0.00210	0.40
29	0.1534	0.9977	0.0126	23.75	0.1537	0.00193	0.36	0.1497	0.00221	0.42
30	0.1587	0.9969	0.0120	22.68	0.1592	0.00192	0.36	0.1548	0.00214	0.40

Standard deviations are given in mm and pixels.

Table 6 – Variance in measurement of drawn line dimensions

(A)	Length			Diameter			
	WR	DT	IP	WR (average)	WR (calculated)	DT	IP
(A) 189 px mm^{-1}, 20 pixel thick, 9.983 mm long lines rotated in 1° increments							
Mean (mm)	9.96	10.07	10.07	0.106	0.102	0.104	0.105
S.D. (mm)	0.122	1.017	0.080	0.001	0.002	0.001	0.000
S.D (px)	23.04	192.25	15.20	0.246	0.356	0.225	0.053
Diff (mm)	0.025	−0.089	−0.086	0.000	0.004	0.002	0.001
Diff (px)	4.73	−16.74	−16.28	−0.059	0.682	0.376	0.099
Range (mm)	0.436	3.283	0.337	0.005	0.005	0.005	0.001
Range (px)	82.42	620.66	63.73	0.888	1.009	0.959	0.204

(B)	IP (19)	IP (20)
(B) 189 px mm^{-1}, 19 and 20 pixel thick lines rotated in 5° increments		
Mean (mm)	0.0994	0.1054
S.D. (mm)	0.0033	0.0003
S.D (px)	0.6260	0.0489

Length and diameter measurements for all three packages ($n = 46$) (S.D. is the standard deviation of the values, diff the difference between actual value and mean value; range the difference between the maximum and minimum values; mm = millimeters). Width calculations for Image Processing Tool Kit, to show the even vs. odd pixel width differences ($n = 9$).

Table 7 – Table comparing caliper measured diameters with WinRhizo measured diameter and length

Measured width (mm)										
Individual wires			0.193	0.245	0.254	0.448	0.506	0.580	0	0.653
Gap between wire diameters			0.051	0.009	0.194	0.059	0.074	0	0.072	
	Resolution		In mm							
	px mm^{-1}	mm px^{-1}								
WR diameter										
Individual	94	0.011	0.186	0.238	0.248	0.437	0.485	0.542	0	0.636
Mixture	24	0.042	0.198	0	0	0.448	0	0	0	0.607
	47	0.021	0.207	0	0	0.441	0	0.542	0	0.622
	94	0.011	0.178	0.229	0	0.428	0.481	0.560	0.609	0.631
	142	0.007	0.180	0.222	0.239	0.434	0.483	0.568	0.612	0.634
	189	0.005	0.181	0.223	0.240	0.435	0.482	0.568	0.611	0.633
	Resolution		In cm							Total length (cm)
	px mm^{-1}	mm px^{-1}								
WR length										
Individual	94	0.011	6.5	8.2	7.4	4.9	3.7	3.4	0	7.3	41.4
Mixture	24	0.042	21.8	0	0	11.3	0	0	0	7.6	40.7
	47	0.021	21.6	0	0	8.6	0	3.1	0	6.9	40.2
	94	0.011	6.1	15.1	0	4.7	4.4	2.2	2.8	4.3	39.5
	142	0.007	6.1	6.7	8.2	4.7	3.8	2.0	3.4	3.6	38.4
	189	0.005	6.0	6.5	8.4	4.6	3.8	1.9	2.7	4.2	38.1

"Individual" is WR measurements for parallel wires grouped by diameter. "Mixture" is the full set of wires mixed together and scanned at different resolutions without disturbing the wire arrangement. There were seven measured wire groups, the largest wires were oblong (flattened) rather than cylindrical.

flicts with the observation that the dips in the curves occur every 3–4 pixel (occasionally two and five) widths along the x-axis. Close observation (not shown) of the data and histograms from which Figs. 4a and 5a were derived suggests that these dips occur because of the lack of uniformity in the pattern of width decrease with increasing angle among width classes. The presence of dips at 8 and 12 pixel widths for 94 px mm^{-1} for the line data (Fig. 6) and the legume data (Fig. 9), and at 16 and 23 pixel widths with the 189 px mm^{-1} line data (Fig. 2) strongly supports the supposition that the dips are artifacts that are generated by the algorithm(s) of WR, and not the scanner or the images (one reviewer has suggested a faulty random number generator). The threshold response demonstrated in Fig. 9 demonstrates that these artifacts are independent of threshold based image manipulations.

When an analysis compares treatment effects on the diameter distributions of species where the diameter shifts with changes in treatment (e.g. *Dactylis glomerata* (L) in Ryser, 1998; Zobel et al., 2007), the use of non-linear regression can effectively remove these dips, and allow detection of diameter shifts (Fig. 10). On the other hand, if the response is the initiation of a new diameter class of root (e.g. *Brachypodium pinnatum* (L) Beauv.; Ryser, 1998), non-linear regression will not be useful. The regression analysis will often ignore the dip in curve height at the interface between the two peaks as just another artifact. In addition, if the new diameter peak is relatively narrow, i.e. 4–8 pixels wide, it will likely have a dip in the middle, suggesting two different diameter classes or obscuring the average diameter class. The artifacts (dips), therefore, reduce

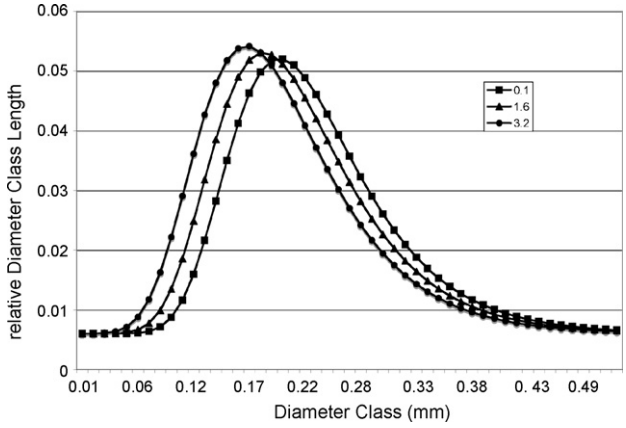

Fig. 10 – Histogram of modeled data for Calopo (tropical legume) roots grown with three different concentrations of phosphorus (0.1, 1.6 and 3.2 mM). The raw data was fitted with non-linear regression and the resultant modeled data points placed in the histogram.

the likelihood of identifying new peaks like that suggested in the *B. pinnatum* histograms (Ryser, 1998).

5. Conclusion

It must be concluded that neither the available image analysis software nor the scanning equipment is currently capable

of documenting fine root diameter shifts of 10% for roots smaller than 0.12 mm diameter. With the artifacts observed in all three software packages (Fig. 2) and a wide range of resolutions (24–400 px mm^{-1}), it is necessary to use non-linear regression techniques to demonstrate any diameter shifts, even with roots in the greater than 0.15 mm diameter range (Figs. 8 and 10). Documentation of the initiation of one or more new diameter classes of root in response to treatments is problematic unless the software is improved. The results with Image Processing Tool Kit analysis of even pixel width lines suggest that it is possible to eliminate these artifacts and observed variances with appropriate algorithms.

REFERENCES

Böhm, W., 1979. Methods of Studying Root Systems. Springer–Verlag, Heidelberg, Germany, p. 188.

Bouma, T.J., Nielsen, K.L., Koutstaal, B., 2000. Sample preparation and scanning protocol for computerized analysis of root length and diameter. Plant Soil 218, 185–196.

Cahn, M.D., Zobel, R.W., Bouldin, D.R., 1989. Relationship between root elongation rate and diameter and duration of growth of lateral roots of maize. Plant Soil 119, 271–279.

Costa, C., Dwyer, L.M., Hamel, C., Muamba, D.F., Wang, X.L., Nantais, L., Smith, D.L., 2001. Root contrast enhancement for measurement with optical scanner-based image analysis. Can. J. Bot. 79, 23–29.

Himmelbauer, M.L., Loiskandl, W., Kastanek, F., 2004. Estimating length, average diameter and surface area of roots using two different Image analyses systems. Plant Soil 260, 111–120.

Kaspar, T.C., Ewing, R.P., 1997. Rootedge: software for measuring root length from desktop scanner images. Agron. J. 89, 932–940.

Lyford, W.H., 1975. Rhizography of non-woody roots of trees in the forest floor. In: Torrey, J.G., Clarkson, D.T. (Eds.), The Development and Function of Roots. Academic Press, London, UK, pp. 179–196.

McPhee, K., 2005. Variation for seedling root architecture in the core collection of pea germplasm. Crop Sci. 45, 1758–1763.

McCully, M.E., 1987. Selected aspects of the structure and development of field-grown roots with special reference to maize. In: Gregory, P.J., Lake, J.V., Rose, D.A. (Eds.), Root Development and Function. Cambridge University Press, Cambridge, UK, pp. 53–70.

Ryser, P., 1998. Intra- and interspecific variation in root length, root turnover and the underlying parameters. In: Lambers, H., Poorter, H., VanVuuren, M.M.I. (Eds.), Inherent Variation in Plant Growth, Physiological Mechanisms and Ecological Consequences. Backhuys Publishers, Leiden, The Netherlands, pp. 441–465.

Ryser, P., Lambers, H., 1996. Root and leaf attributes accounting for the performance of fast- and slow-growing grasses at different nutrient supply. Plant Soil 170, 251–265.

Varney, G.T., Canny, M.J., Wang, X.L., McCully, M.E., 1991. The branch roots of Zea. I. First order branches, their number, sizes and division into classes. Ann. Bot. 67, 357–364.

Wright, S.R., Jennette, M.W., Coble, H.D., Rufty, T.W., 1999. Root morphology of young *Glycine max*, *Senna obtusifolia*, and *Amaranthus palmeri*. Weed Sci. 47, 706–711.

Zobel, R.W., 2003. Sensitivity analysis of computer based diameter measurement from digital images. Crop Sci. 43, 583–591.

Zobel, R.W., 2005. Tertiary root systems. In: Zobel, R.W., Wright, S.F. (Eds.), Roots and Soil Management: Interactions between Roots and the Soil, vol. 48. Agronomy Society of America, Madison, pp. 35–56, Agronomy Monographs.

Zobel, R.W., Alloush, G.A., Belesky, D.P., 2006. Differential root morphology response to no versus high phosphorus in three hydroponically grown forage chicory cultivars. Environ. Exp. Bot. 57, 201–208.

Zobel, R.W., Baligar, V.C., Kinraide, T.B., 2007. Fine root diameters can change in response to changes in nutrient concentrations. Plant Soil 297, 243–254.